

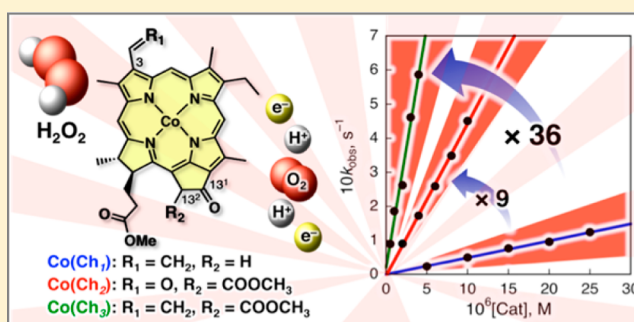
Much Enhanced Catalytic Reactivity of Cobalt Chlorin Derivatives on Two-Electron Reduction of Dioxygen to Produce Hydrogen Peroxide

Kentaro Mase, Kei Ohkubo, and Shunichi Fukuzumi*

Department of Material and Life Science, Graduate School of Engineering, ALCA, Japan Science and Technology Agency (JST), Osaka University, Suita, Osaka 565-0871, Japan

Supporting Information

ABSTRACT: Effects of changes in the redox potential or configuration of cobalt chlorin derivatives ($\text{Co}^{\text{II}}(\text{Ch}_n)$ ($n = 1-3$)) on the catalytic mechanism and the activity of two-electron reduction of dioxygen (O_2) were investigated based on the detailed kinetic study by spectroscopic and electrochemical measurements. Nonsubstituted cobalt chlorin complex ($\text{Co}^{\text{II}}(\text{Ch}_1)$) efficiently and selectively catalyzed two-electron reduction of dioxygen (O_2) by a one-electron reductant (1,1'-dimethylferrocene) to produce hydrogen peroxide (H_2O_2) in the presence of perchloric acid (HClO_4) in benzonitrile (PhCN) at 298 K. The detailed kinetic studies have revealed that the rate-determining step in the catalytic cycle is the proton-coupled electron transfer reduction of O_2 with the protonated $\text{Co}^{\text{II}}(\text{Ch}_1)$ complex ($[\text{Co}^{\text{II}}(\text{Ch}_1\text{H})]^+$), where one-electron reduction potential of $[\text{Co}^{\text{III}}(\text{Ch}_1)]^+$ was changed from 0.37 V (vs SCE) to 0.48 V by the addition of HClO_4 due to the protonation of $[\text{Co}^{\text{III}}(\text{Ch}_1)]^+$. The introduction of electron-withdrawing aldehyde group (position C-3) ($\text{Co}^{\text{II}}(\text{Ch}_3)$) and both methoxycarbonyl group (position C-13²) and aldehyde group (position C-3) ($\text{Co}^{\text{II}}(\text{Ch}_2)$) on the chlorin ligand resulted in the positive shifts of redox potential for $\text{Co}(\text{III}/\text{II})$ from 0.37 V to 0.45 and 0.40 V, respectively, whereas, in the presence of HClO_4 , no positive shifts of those redox potentials for $[\text{Co}^{\text{III}}(\text{Ch}_n)]^+/\text{Co}^{\text{II}}(\text{Ch}_n)$ ($n = 2, 3$) were observed due to lower acceptability of protonation. As a result, such a change in redox property resulted in the enhancement of the catalytic reactivity, where the observed rate constant (k_{obs}) value of $\text{Co}^{\text{II}}(\text{Ch}_3)$ was 36-fold larger than that of $\text{Co}^{\text{II}}(\text{Ch}_1)$.



INTRODUCTION

Efficient conversion of electrical energy produced by solar cells into easily storable energy has attracted increasing attention as a key technology for the practical use of solar energy.^{1,2} Hydrogen peroxide (H_2O_2) produced by two-electron reduction of earth abundant dioxygen (O_2) is a promising candidate as a high chemical energy carrier, because it has high energy density owing to its liquid state at ambient temperature.³ H_2O_2 stored as high chemical energy can be transformed into electrical energy through fuel cells.³⁻⁸ H_2O_2 -fuel cell supplies theoretical output voltage of 1.09 V by utilizing H_2O_2 as both a fuel at cathode and an oxidant at anode, emitting only water and oxygen after power generation, and its cell performance has been improved significantly.³⁻⁸ Currently, H_2O_2 is produced in industry mainly by the anthraquinone method, in which H_2O_2 is produced in the process of the autoxidation of a 2-alkylanthrahydroquinone to the corresponding anthraquinone.⁹ However, this process requires hydrogen as a reducing reagent and a noble metal such as palladium to regenerate the anthrahydroquinone. The cost of the anthraquinone process depends heavily on effective recycling of the anthraquinone, extraction solvents, and noble metal catalysts for the hydrogenation, which are all quite expensive.

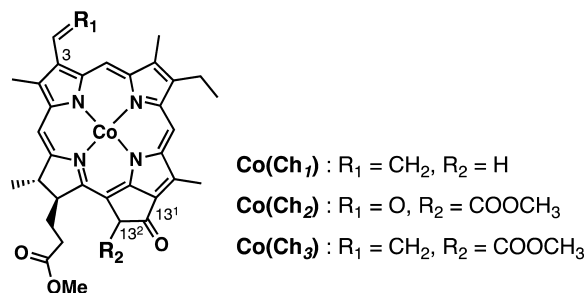
In order to resolve these matters, an alternative method to produce H_2O_2 has been extensively studied by photochemical or thermal means without the use of noble metal catalysts.¹⁰⁻¹⁷ Extensive efforts have been implemented based on homogeneous transition metal complexes such as cobalt,¹⁸⁻²⁸ iron,²⁹⁻³² and copper,³³⁻³⁶ and other metal complexes¹⁷ have been employed for the two-electron and four-electron reduction of O_2 . So far, monomeric cobalt-centered complexes have been reported to show high affinity for the O_2 reduction and act as efficient catalysts for the selective two-electron reduction of O_2 to produce H_2O_2 .¹⁸⁻²⁰ Nevertheless, the stability of those catalysts under the acidic conditions was not well taken into account. Decomposition of metal complexes with a porphyrinoid ligand is mainly caused by demetalation of metal center in an acidic medium, which depends on two factors.³⁷⁻⁴⁰ One is the core size and rigidity of a macrocyclic ligand, because a low-valent metal ion, which is produced in a catalytic cycle, is difficult to be accommodated in a macrocyclic ligand due to its large ionic radius and low electrostatic interaction. The other is the nucleophilicity of core nitrogen atoms, which is responsible for the replacement of the metal ion by incoming proton.

Received: November 11, 2014

We have previously reported that a cobalt chlorin complex ($\text{Co}^{\text{II}}(\text{Ch})$) efficiently and selectively catalyzes two-electron reduction of O_2 by using one-electron molecular reductants (ferrocene derivatives) with high catalyst stability and small overpotential in the presence of perchloric acid (HClO_4) in benzonitrile (PhCN).¹⁸ The remarkable stability and efficiency are attributed to the nature of chlorin ligand; the core size of the ligand is larger and more flexible than that of porphyrin ligand, and lower basicity of the core nitrogen atoms is induced by the protonation of the carbonyl group (position C-13¹) to prevent protonation of core nitrogen atoms. In addition, the chemical reduction approach under homogeneous conditions allows the survey of the catalytic mechanism, where the rate-determining step was determined to be proton-coupled electron transfer (PCET) from $\text{Co}^{\text{II}}(\text{Ch}_1)$ to O_2 .¹⁸ However, effects of changes in the redox potential and configuration of chlorin ligand on the catalytic activity have yet to be examined to further improve the catalytic activity.

We report much enhanced catalytic activity of cobalt chlorin complexes for selective two-electron reduction of O_2 to H_2O_2 by examining a series of cobalt chlorin derivatives, $\text{Co}^{\text{II}}(\text{Ch}_n)$ ($n = 1-3$), shown in Chart 1. The detailed study based on the

Chart 1. Cobalt Chlorin Derivatives



kinetics and thermodynamics have provided valuable insight into the development of a more efficient electrocatalyst for two-electron reduction of O_2 to H_2O_2 , which is essential to realize a H_2O_2 -energy society.

EXPERIMENTAL SECTION

General Procedure. Chemicals were purchased from commercial sources and used without further purification, unless otherwise noted. Benzonitrile (PhCN) used for spectroscopic and electrochemical measurements was distilled over phosphorus pentoxide prior to use.⁴¹ Cobalt chlorin [$\text{Co}^{\text{II}}(\text{Ch}_n)$, $n = 1-3$] was synthesized by the published method (see ref 18 for the details).⁴²⁻⁴⁵ 1,1'-Dimethylferrocene (Me_2Fc) were purchased from Aldrich Chemical Co. and purified by sublimation or recrystallization from ethanol. Tetra-*n*-butylammonium hexafluorophosphate (TBAPF_6) purchased from Wako Pure Chemical Industries, Ltd., was twice recrystallized from ethanol and dried *in vacuo* prior to use. ^1H NMR spectra (300 MHz) were recorded on a JEOL AL-300 spectrometer at room temperature, and chemical shifts (ppm) were determined relative to tetramethylsilane (TMS). MALDI-TOF-MS measurements were performed on a Kratos Compact MALDI I (Shimadzu) using freshly prepared dithranol as a matrix in the reflectron-positive mode. UV-vis spectroscopy was carried out on a Hewlett-Packard 8453 diode array spectrophotometer at room temperature using a quartz cell (light path length = 1 cm).

Spectroscopic Measurements. Titrations were carried out by adding known quantities of a solution of HClO_4 in high concentration into a solution of $\text{Co}^{\text{II}}(\text{Ch}_n)$. The solution of HClO_4 used to effect the titration contained the same concentration of $\text{Co}^{\text{II}}(\text{Ch}_n)$ as used in the titration so as to avoid the need to account for dilution effects during the titration. The protonation equilibrium constant between $\text{Co}(\text{Ch}_n)$

and $[\text{Co}(\text{Ch}_n\text{H})]^+$ was determined by using the Hill equation, which analyzes changes of absorption spectra during the titration as a function of concentration of an added acid.⁴⁶ The amount of hydrogen peroxide (H_2O_2) formed was determined by titration with iodide ion: A diluted CH_3CN solution (2.0 mL) of the product mixture (40 μL) was treated with an excess amount of NaI, and the amount of I_3^- formed was determined by the absorption spectrum ($\lambda_{\text{max}} = 361 \text{ nm}$, $\epsilon = 2.8 \times 10^4 \text{ M}^{-1} \text{ cm}^{-1}$).⁴⁷

Kinetic Measurements. Rate constants of oxidation of ferrocene derivatives by O_2 in the presence of a catalytic amount of $\text{Co}^{\text{II}}(\text{Ch}_n)$ ($n = 1-3$) and an excess amount of HClO_4 in PhCN at 298 K were determined by monitoring the appearance of an absorption band due to 1,1'-dimethylferrocenium ion (Me_2Fc^+ ; $\lambda_{\text{max}} = 650 \text{ nm}$, $\epsilon_{\text{max}} = 290 \text{ M}^{-1} \text{ cm}^{-1}$).¹⁵ At the wavelengths monitored, spectral overlap was observed with $[\text{Co}^{\text{II}}(\text{Ch}_1\text{H})]^+$ [$\lambda = 650 \text{ nm}$ ($1.4 \times 10^4 \text{ M}^{-1} \text{ cm}^{-1}$), 700 nm ($7.0 \times 10^3 \text{ M}^{-1} \text{ cm}^{-1}$)], $[\text{Co}^{\text{II}}(\text{Ch}_2\text{H})]^+$ [$\lambda = 650 \text{ nm}$ ($\epsilon = 8.5 \times 10^3 \text{ M}^{-1} \text{ cm}^{-1}$), 700 nm ($\epsilon = 1.0 \times 10^4 \text{ M}^{-1} \text{ cm}^{-1}$)], and $[\text{Co}^{\text{II}}(\text{Ch}_3\text{H})]^+$ [$\lambda = 650 \text{ nm}$ ($\epsilon = 1.2 \times 10^4 \text{ M}^{-1} \text{ cm}^{-1}$), 700 nm ($\epsilon = 5.0 \times 10^3 \text{ M}^{-1} \text{ cm}^{-1}$)]. An air-saturated PhCN solution was used for the catalytic reduction of O_2 by Me_2Fc . The concentration of O_2 in an air-saturated PhCN solution ($1.7 \times 10^{-3} \text{ M}$) was determined as reported previously.⁴⁸ The concentrations of Me_2Fc employed for the catalytic reduction of O_2 were much larger than that of O_2 , when O_2 is the reaction-limiting reagent in the reaction solution. The catalytic turnover numbers (TON = mol of H_2O_2 as the product of the two-electron reduction of O_2 /mol of $\text{Co}^{\text{II}}(\text{Ch}_n)$, $n = 1-3$) were determined based on the initial concentration of $\text{Co}^{\text{II}}(\text{Ch}_n)$, when the concentrations of $\text{Co}^{\text{II}}(\text{Ch}_n)$, Me_2Fc , and HClO_4 in O_2 -saturated PhCN were $1.0 \times 10^{-7} \text{ M}$, $5.0 \times 10^{-2} \text{ M}$, and $5.0 \times 10^{-2} \text{ M}$, respectively. The formation of Me_2Fc^+ was monitored by a rise in absorbance at 700 nm to avoid excess absorption at 650 nm.

Electrochemical Measurements. Cyclic voltammetry (CV) measurements were performed on an ALS 630B electrochemical analyzer, and voltammograms were measured in deaerated PhCN containing TBAPF_6 (0.10 M) as a supporting electrolyte at room temperature. A conventional three-electrode cell was used with a glassy carbon working electrode (surface area of 0.3 mm^2) and a platinum wire as the counter electrode. The glassy carbon working electrode (BAS) was routinely polished with BAS polishing alumina suspension and rinsed with acetone before use. The potentials were measured with respect to the Ag/AgNO_3 ($1.0 \times 10^{-2} \text{ M}$) reference electrode. All potentials (vs Ag/AgNO_3) were converted to values vs saturated calomel electrode (SCE) by adding 0.29 V.⁴⁹ Redox potentials were determined using the relation $E_{1/2} = (E_{\text{pa}} + E_{\text{pc}})/2$.

EPR Measurements. The EPR spectra were performed on a JEOL X-band EPR spectrometer (JES-ME-LX) using a quartz EPR tube containing a deaerated frozen sample solution at 4 K. The internal diameter of the EPR tube is 4.5 mm, which is small enough to fill the EPR cavity but large enough to obtain good signal-to-noise ratios during the EPR measurements at low temperature. The EPR spectra were measured under nonsaturating microwave power conditions. The amplitude of modulation was chosen to optimize the resolution and the signal-to-noise (S/N) ratio of the observed spectra. The g values were calibrated with a Mn^{2+} marker.

RESULTS AND DISCUSSION

Protonation of $\text{Co}^{\text{II}}(\text{Ch}_n)$, $n = 1-3$. To examine the proton acceptability of $\text{Co}^{\text{II}}(\text{Ch}_n)$, acid titration was performed in PhCN by means of UV-vis spectroscopy. The protonation equilibrium constants (K) of $\text{Co}^{\text{II}}(\text{Ch}_n)$ with HClO_4 were determined by monitoring absorption spectral change at Q-bands of $\text{Co}^{\text{II}}(\text{Ch}_n)$ upon addition of HClO_4 to deaerated PhCN solutions of $\text{Co}^{\text{II}}(\text{Ch}_n)$ at 298 K. The Q bands of $\text{Co}^{\text{II}}(\text{Ch}_2)$ at 675 nm decreased with increasing concentration of HClO_4 , followed by appearance of a broaden absorption band at 678 nm as shown Figure 1. Such a UV-vis absorption spectral change with clean isosbestic points has previously been analyzed as monoprotinated at the carbonyl group (position

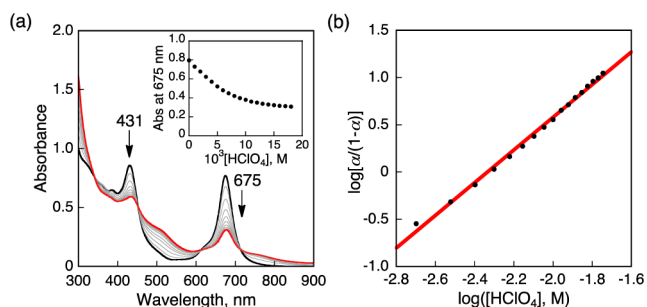
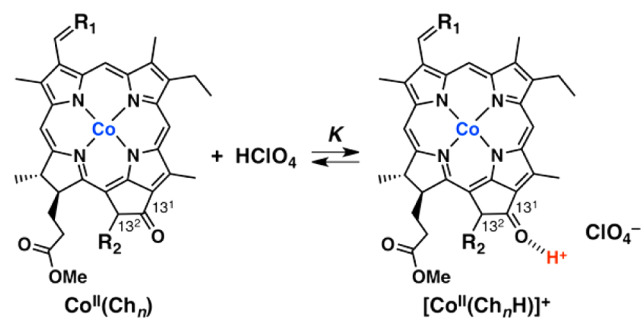


Figure 1. (a) Absorption spectral changes in the protonation of $\text{Co}^{\text{II}}(\text{Ch}_2)$ (2.0×10^{-5} M) upon addition of HClO_4 to a deaerated PhCN solution of $\text{Co}^{\text{II}}(\text{Ch}_2)$ at 298 K. Inset shows absorbance change at 675 nm upon addition of HClO_4 . (b) Hill plot of absorbance change at 675 nm upon addition of HClO_4 , where α is $(A - A_0)/(A_\infty - A_0)$.

C-13^1) to form $[\text{Co}^{\text{II}}(\text{Ch}_n\text{H})]^+$ ($n = 1-3$), as shown in Scheme 1.¹⁸

Scheme 1. Protonation of $\text{Co}^{\text{II}}(\text{Ch}_n)$, $n = 1-3$



The K value for the monoprotection of $\text{Co}^{\text{II}}(\text{Ch}_2)$ was determined to be $2.2 \times 10^2 \text{ M}^{-1}$ in deaerated PhCN at 298 K. Likewise, the addition of HClO_4 to a solution of $\text{Co}^{\text{II}}(\text{Ch}_3)$ afforded similar spectral changes as shown in Figure S4 in the Supporting Information. However, higher concentration of HClO_4 was required to obtain monoprotected $\text{Co}^{\text{II}}(\text{Ch}_3)$ as compared with that of $\text{Co}(\text{Ch}_2)$. The relatively smaller K values of $\text{Co}^{\text{II}}(\text{Ch}_3)$ were determined to be 70 M^{-1} as listed in Table 1. These K values of $\text{Co}^{\text{II}}(\text{Ch}_n)$ ($n = 2, 3$) are much smaller

Table 1. Protonation Equilibrium Constants of $\text{Co}^{\text{II}}(\text{Ch}_n)$ and $[\text{Co}^{\text{III}}(\text{Ch}_n)]^+$ ($n = 1-3$) Measured at 298 K

cobalt chlorin	K, M^{-1}	
	Co(II)	Co(III)
$\text{Co}^{\text{II}}(\text{Ch}_1)$	2.2×10^{4a}	1.2×10^{2a}
$\text{Co}^{\text{II}}(\text{Ch}_2)$	2.2×10^2	b
$\text{Co}^{\text{II}}(\text{Ch}_3)$	7.0×10	b

^aData taken from ref 18. ^bNo protonation.

than the K value of $\text{Co}^{\text{II}}(\text{Ch}_1)$ ($K = 2.2 \times 10^4 \text{ M}^{-1}$)¹⁸ because of a decrease in the electron density of macrocyclic ligands caused by the introduction of electron-withdrawing substituents, such as methoxycarbonyl group (position C-13²) and aldehyde group (position C-3), as expected from the weaker basicity of macrocyclic ligands with the electron-withdrawing substituents as compared to the basicity of unsubstituted macrocyclic ligand. The methoxycarbonyl group (position C-13²) near by the carbonyl group (position C-13¹) may also cause steric hindrance, preventing the approach of proton with

bulky ClO_4^- counter anion to the carbonyl group (position C-13¹).

The protonation of $\text{Co}^{\text{II}}(\text{Ch}_n)$ ($n = 1-3$) at the carbonyl group (position C-13¹) was previously evidenced by the changes in EPR spectra, where the g_{\parallel} value remained nearly the same, whereas the g_{\perp} value changed slightly upon addition of HClO_4 to deaerated PhCN solutions of $\text{Co}^{\text{II}}(\text{Ch}_n)$ ($n = 1-3$) at 4 K.¹⁸ The larger changes in g values were observed for the protonation of $\text{Co}^{\text{II}}(\text{Ch}_1)$ as compared to those of $\text{Co}^{\text{II}}(\text{Ch}_n)$ ($n = 2, 3$), as shown in Figure 2.

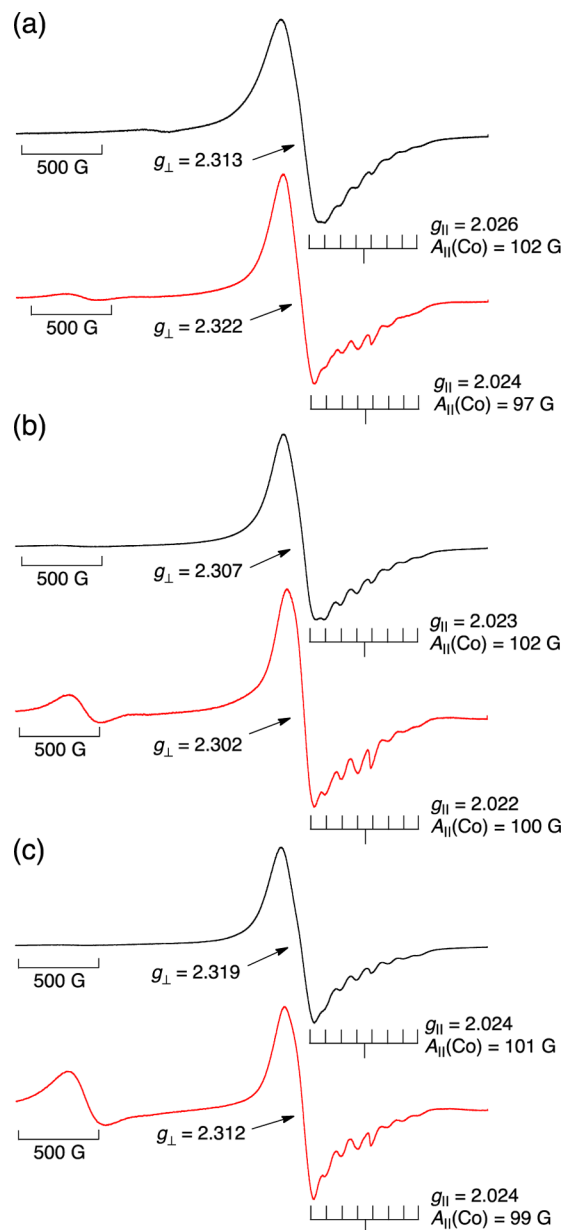
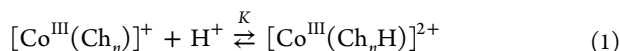


Figure 2. EPR spectra of (a) $\text{Co}^{\text{II}}(\text{Ch}_1)$ (1.0×10^{-3} M) in deaerated PhCN at 4 K (black) and $\text{Co}^{\text{II}}(\text{Ch}_1)$ (1.0×10^{-3} M) upon addition of HClO_4 (1.0×10^{-2} M) in deaerated PhCN at 4 K (red), (b) $\text{Co}^{\text{II}}(\text{Ch}_2)$ (1.0×10^{-3} M) in deaerated PhCN at 4 K (black) and $\text{Co}^{\text{II}}(\text{Ch}_2)$ (1.0×10^{-3} M) upon addition of HClO_4 (1.0×10^{-2} M) in deaerated PhCN at 4 K (red), and (c) $\text{Co}^{\text{II}}(\text{Ch}_3)$ (1.0×10^{-3} M) in deaerated PhCN at 4 K (black) and $\text{Co}^{\text{II}}(\text{Ch}_3)$ (1.0×10^{-3} M) upon addition of HClO_4 (1.0×10^{-2} M) in deaerated PhCN at 4 K (red).

The same set of spectral titrations was performed on one-electron oxidized species, $[\text{Co}^{\text{III}}(\text{Ch}_n)]^+$ ($n = 1-3$), produced by aerial oxidation of $\text{Co}^{\text{II}}(\text{Ch}_n)$ in the presence of a small amount of HClO_4 . As can be seen in the previous report,¹⁸ the protonation equilibrium constants (K) of $[\text{Co}^{\text{III}}(\text{Ch}_n)]^+$ ($n = 1-3$), as given by eq 1, exhibited much smaller values due to lower basicity of chlorin ligand induced by the higher-valent Co(III) ion center, as shown in Figure S5 in the Supporting Information.



The K value for the monoprotation of $[\text{Co}^{\text{III}}(\text{Ch}_1)]^+$ was previously determined to be $1.2 \times 10^2 \text{ M}^{-1}$ in air-saturated PhCN at 298 K. However, the addition of HClO_4 to an air-saturated PhCN solution of $[\text{Co}^{\text{III}}(\text{Ch}_n)]^+$ ($n = 2, 3$) resulted in virtually no spectral change, where K values could not be determined. The protonation equilibrium constants between $\text{Co}^{\text{II}}(\text{Ch}_n)$ and $[\text{Co}^{\text{II}}(\text{Ch}_n\text{H})]^+$ together with $[\text{Co}^{\text{III}}(\text{Ch}_n)]^+$ and $[\text{Co}^{\text{III}}(\text{Ch}_n\text{H})]^{2+}$ as given by Scheme 1 and eq 1 are listed in Table 1.

Redox Properties of $\text{Co}^{\text{II}}(\text{Ch}_n)$, $n = 1-3$. Electrochemical measurements of cobalt(II) chlorin derivatives were measured to examine the influence of the substituents of chlorin macrocyclic ligands on the catalytic activity. The cyclic voltammograms for all the $\text{Co}^{\text{II}}(\text{Ch}_n)$ in deaerated PhCN solutions containing TBAPF₆ (0.10 M) exhibited reversible two-oxidation waves for conversion of $\text{Co}^{\text{II}}(\text{Ch}_n)$ to $[\text{Co}^{\text{III}}(\text{Ch}_n)]^+$ and $[\text{Co}^{\text{III}}(\text{Ch}_n)]^+$ to $[\text{Co}^{\text{III}}(\text{Ch}_n^{\bullet+})]^{2+}$, respectively, as shown in Figure 3.

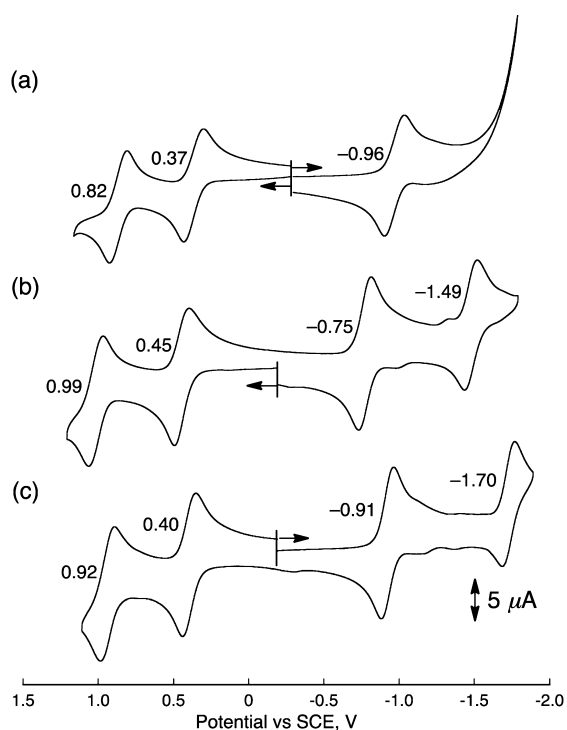


Figure 3. Cyclic voltammograms of deaerated PhCN solutions of (a) $\text{Co}^{\text{II}}(\text{Ch}_1)$ ($2.0 \times 10^{-3} \text{ M}$), (b) $\text{Co}^{\text{II}}(\text{Ch}_2)$ ($2.0 \times 10^{-3} \text{ M}$), and (c) $\text{Co}^{\text{II}}(\text{Ch}_3)$ ($2.0 \times 10^{-3} \text{ M}$) recorded in the presence of TBAPF₆ (0.10 M) at 298 K, respectively; sweep rate: 0.10 V s^{-1} .

In contrast to oxidation sweep, reduction sweep for $\text{Co}^{\text{II}}(\text{Ch}_1)$ shows one-reduction waves whereas reduction

sweeps for $\text{Co}^{\text{II}}(\text{Ch}_2)$ and $\text{Co}^{\text{II}}(\text{Ch}_3)$ show two-reduction waves. On the basis of redox potentials of previously characterized Co(II) porphyrins,⁵⁰ the first reduction processes are assigned as due to formation of the Co(I) complex, $[\text{Co}^{\text{I}}(\text{Ch}_1)]^-$. Additionally, $\text{Co}^{\text{II}}(\text{Ch}_2)$ and $\text{Co}^{\text{II}}(\text{Ch}_3)$ undergo the second reduction ascribed to one-electron ligand reduction to form Co(I) radical anion complex $[\text{Co}^{\text{I}}(\text{Ch}_n^{\bullet-})]^{2-}$, $n = 2, 3$. Each redox couple was positively shifted from 0.37 V (vs SCE) for $[\text{Co}^{\text{III}}(\text{Ch}_1)]^+/\text{Co}^{\text{II}}(\text{Ch}_1)$ to 0.40 V for $[\text{Co}^{\text{III}}(\text{Ch}_3)]^+/\text{Co}^{\text{II}}(\text{Ch}_3)$ and 0.45 V for $[\text{Co}^{\text{III}}(\text{Ch}_2)]^+/\text{Co}^{\text{II}}(\text{Ch}_2)$, respectively. Those are explained by the introduction of electron-withdrawing methoxycarbonyl group (position C-13²) or both methoxycarbonyl group (position C-13²) and aldehyde group (position C-3).

Upon addition of HClO_4 to the deaerated $[\text{Co}^{\text{III}}(\text{Ch}_n)]^+$ solutions, the redox potential of $[\text{Co}^{\text{III}}(\text{Ch}_1)]^+/\text{Co}^{\text{II}}(\text{Ch}_1)$ was positively shifted from 0.37 to 0.48 V, whereas the redox potential of $[\text{Co}^{\text{III}}(\text{Ch}_n)]^+/\text{Co}^{\text{II}}(\text{Ch}_n)$ ($n = 2, 3$) remained the same as that in the absence of HClO_4 (Figure 4).

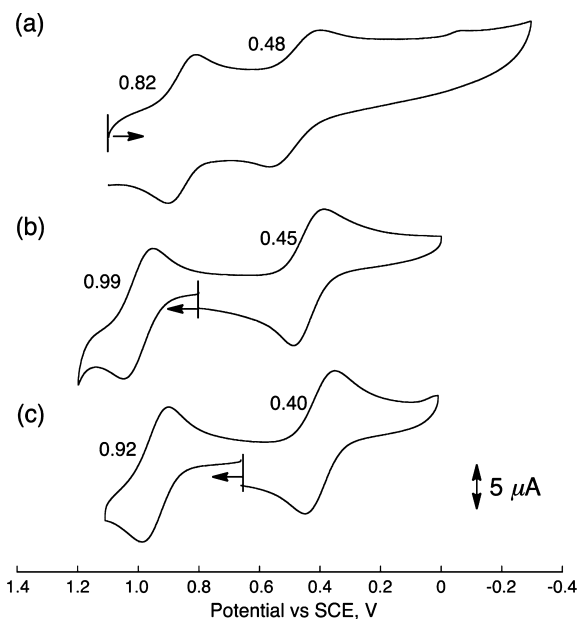


Figure 4. Cyclic voltammograms of deaerated PhCN solutions of (a) $\text{Co}^{\text{II}}(\text{Ch}_1)$ ($2.0 \times 10^{-3} \text{ M}$), (b) $\text{Co}^{\text{II}}(\text{Ch}_2)$ ($2.0 \times 10^{-3} \text{ M}$), and (c) $\text{Co}^{\text{II}}(\text{Ch}_3)$ ($2.0 \times 10^{-3} \text{ M}$) with HClO_4 ($2.5 \times 10^{-2} \text{ M}$) recorded in the presence of TBAPF₆ (0.10 M) at 298 K, respectively; sweep rate: 0.10 V s^{-1} .

These results are consistent with the observation that the ligand protonation hardly occurred on $\text{Co}^{\text{II}}(\text{Ch}_n)$ ($n = 2, 3$) due to diminished basicity and steric hindrance on chlorin ligand caused by the introduction of substituents. Table 2 summarizes all the redox potentials of $[\text{Co}^{\text{III}}(\text{Ch}_n)]^+/\text{Co}^{\text{II}}(\text{Ch}_n)$ ($n = 1-3$)

Table 2. Redox Potentials (V vs SCE) of $\text{Co}^{\text{III}}/\text{Co}^{\text{II}}$ in the Absence and Presence of HClO_4 Measured at 298 K

cobalt chlorin	$E_{1/2}$ of $\text{Co}^{\text{III}}/\text{Co}^{\text{II}}$, V	
	without HClO_4	with 25 mM of HClO_4
$\text{Co}^{\text{II}}(\text{Ch}_1)$	0.37	0.48
$\text{Co}^{\text{II}}(\text{Ch}_2)$	0.45	0.45
$\text{Co}^{\text{II}}(\text{Ch}_3)$	0.40	0.40

^aData taken from ref 18.

in the absence and presence of HClO_4 . Consequently, the oxidation potential of $\text{Co}^{\text{II}}(\text{Ch}_1)$, where the $\text{Co}(\text{II})$ complexes are responsible for the rate-determining O_2 reduction step in the catalytic cycle as reported previously, turned out to be the highest value in the presence of HClO_4 .

Catalytic Two-Electron Reduction of O_2 by Me_2Fc with $\text{Co}^{\text{II}}(\text{Ch}_n)$ in the Presence of HClO_4 . Catalytic O_2 reduction under homogeneous conditions was conducted by the addition of 1,1'-dimethylferrocene (Me_2Fc) as a molecular reductant to an air-saturated PhCN solution, containing $\text{Co}^{\text{II}}(\text{Ch}_n)$ ($n = 1-3$) as a catalyst and HClO_4 as a proton source. The efficient oxidation of Me_2Fc by O_2 occurred in the presence of $\text{Co}^{\text{II}}(\text{Ch}_n)$ ($n = 1-3$) to afford 1,1'-dimethylferrocenium ion (Me_2Fc^+) as shown in Figure 5, whereas the oxidation has

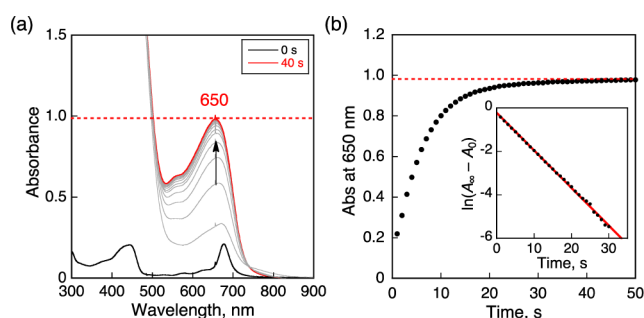
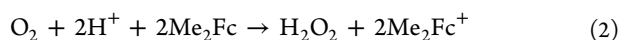


Figure 5. (a) Absorption spectral change in the two-electron reduction of O_2 (1.7×10^{-3} M) by Me_2Fc (2.5×10^{-2} M) with $\text{Co}^{\text{II}}(\text{Ch}_2)$ (4.0×10^{-6} M) in the presence of HClO_4 (2.5×10^{-2} M) in air-saturated PhCN at 298 K. The black and red lines show the spectra before and after addition of HClO_4 , respectively. The dotted line is the absorbance at 650 nm due to 3.4×10^{-3} M of Me_2Fc^+ . (b) Time profile of absorbance at 650 nm due to Me_2Fc^+ . Inset: first-order plot.

hardly occurred in the absence of $\text{Co}^{\text{II}}(\text{Ch}_n)$ ($n = 1-3$) under the same experimental conditions. In order to determine the stoichiometry of the catalytic O_2 reduction with $\text{Co}^{\text{II}}(\text{Ch}_n)$ ($n = 1-3$), the oxidized amount of Me_2Fc by O_2 was quantitatively determined under the reaction conditions with an excess amount of Me_2Fc and HClO_4 relative to the concentration of O_2 (i.e., $[\text{O}_2] \ll [\text{Me}_2\text{Fc}], [\text{HClO}_4]$). A representative example of the UV-vis spectral change in the catalytic reduction of O_2 by Me_2Fc with $\text{Co}^{\text{II}}(\text{Ch}_2)$ is shown in Figure 5, where the formation of Me_2Fc^+ was monitored by a rise in absorbance at 650 nm. The time profile of the formation of Me_2Fc^+ in the reduction of limited concentration of O_2 (1.7×10^{-3} M) is shown in Figure 5b, where two-equivalent of Me_2Fc^+ (3.4×10^{-3} M) to the concentration of O_2 dissolved in PhCN was formed at the end of catalytic reaction. This result indicates that two-electron reduction of O_2 to produce H_2O_2 catalyzed by $\text{Co}^{\text{II}}(\text{Ch}_n)$ ($n = 1-3$) was successfully achieved with nearly 100% selectivity in the PhCN solution, as given by eq 2. The formation of H_2O_2 was confirmed by the iodometric titration (see Experimental Section).



The rate of the formation of Me_2Fc^+ obeyed pseudo-first-order kinetics under the conditions of $[\text{O}_2] \ll [\text{Me}_2\text{Fc}], [\text{HClO}_4]$, suggesting that the oxidation of $\text{Co}^{\text{II}}(\text{Ch}_n)$ by O_2 is rate-determining step and the catalytic rate has first-order dependence on the concentration of O_2 .

Figure 6 presents the comparison of the dependence of observed rate constant (k_{obs}) under the same pseudo-first-order

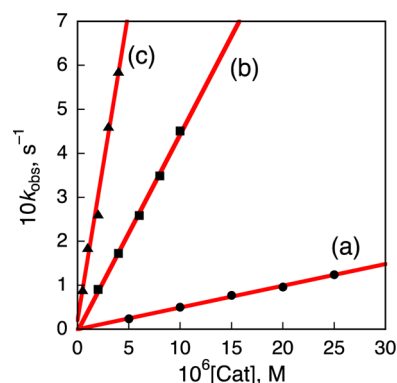


Figure 6. Plots of (a) k_{obs} vs $[\text{Co}^{\text{II}}(\text{Ch}_1)]$ (closed circle), (b) k_{obs} vs $[\text{Co}^{\text{II}}(\text{Ch}_2)]$ (closed square), and (c) k_{obs} vs $[\text{Co}^{\text{II}}(\text{Ch}_3)]$ (closed triangle) for the two-electron reduction of O_2 (1.7×10^{-3} M) by Me_2Fc (2.5×10^{-2} M) in the presence of HClO_4 (2.5×10^{-2} M) in PhCN at 298 K.

conditions for the formation of Me_2Fc^+ on concentrations of a series of catalysts ($\text{Co}^{\text{II}}(\text{Ch}_n)$, $n = 1-3$). The k_{obs} values increased linearly with increasing concentrations of catalysts ($\text{Co}^{\text{II}}(\text{Ch}_n)$, $n = 1-3$). The higher activity was achieved when $\text{Co}^{\text{II}}(\text{Ch}_n)$ ($n = 2, 3$) were employed as catalysts, where the k_{obs} value of $\text{Co}^{\text{II}}(\text{Ch}_2)$ was 9-fold larger than that of $\text{Co}^{\text{II}}(\text{Ch}_1)$ and the k_{obs} value of $\text{Co}^{\text{II}}(\text{Ch}_3)$ was 36-fold larger than that of $\text{Co}^{\text{II}}(\text{Ch}_1)$. The turnover numbers (TON) of $\text{Co}^{\text{II}}(\text{Ch}_n)$ ($n = 1-3$) were determined from the produced concentration of Me_2Fc^+ to be more than 60,000, 79,000, and 83,000 respectively, when small concentrations of catalysts were employed, as shown in Figure S6 in the Supporting Information.

Kinetics and Mechanism of Two-Electron Reduction of O_2 Catalyzed by $\text{Co}^{\text{II}}(\text{Ch}_n)$. The mechanism of catalytic O_2 reduction with $\text{Co}^{\text{II}}(\text{Ch}_n)$ ($n = 2, 3$) was determined by investigating the dependence of the observed rate constant for the formation of Me_2Fc^+ on concentrations of $\text{Co}^{\text{II}}(\text{Ch}_n)$ ($n = 2, 3$), Me_2Fc , HClO_4 , and O_2 .¹⁸ The k_{obs} values increased linearly with increasing concentration of $\text{Co}^{\text{II}}(\text{Ch}_n)$ ($n = 2, 3$) (Figure 6) and O_2 (Figures 7c and S9c in the Supporting Information). In contrast, the k_{obs} values remained constant irrespective of the change in the concentration of Me_2Fc (Figures 7b and S9b in the Supporting Information). However, in the case of $\text{Co}^{\text{II}}(\text{Ch}_n)$ ($n = 2, 3$), plots of k_{obs} values vs the concentration of HClO_4 exhibited a saturation behavior (Figures 7a and S9a in the Supporting Information).⁵¹ Such a saturation behavior of k_{obs} values on the concentration of HClO_4 together with the first-order dependence of k_{obs} values on the concentration of $\text{Co}^{\text{II}}(\text{Ch}_n)$ ($n = 2, 3$) and O_2 is explained by a change in the rate-determining step from proton-coupled electron transfer (PCET) from $\text{Co}^{\text{II}}(\text{Ch}_n)$ ($n = 2, 3$) to O_2 to produce $[\text{Co}^{\text{III}}(\text{Ch}_n)]^+$ ($n = 2, 3$) and HO_2^\bullet to deprotonation of $[\text{Co}^{\text{II}}(\text{Ch}_n\text{H})]^+$ to form $\text{Co}^{\text{II}}(\text{Ch}_n)$ at large concentrations of HClO_4 as shown in Scheme 2.

Thus, the kinetic equation for the reduction of O_2 catalyzed by both $\text{Co}^{\text{II}}(\text{Ch}_2)$ and $\text{Co}^{\text{II}}(\text{Ch}_3)$ is given by eq 3,

$$d[\text{Me}_2\text{Fc}^+]/dt = k_{\text{cat}(n)}[\text{Co}^{\text{II}}(\text{Ch}_n)][\text{O}_2][\text{HClO}_4] \quad (3)$$

where $k_{\text{cat}(n)}$ ($n = 2, 3$) is catalytic rate constant with $\text{Co}^{\text{II}}(\text{Ch}_n)$ ($n = 2, 3$). From the protonation equilibrium between $\text{Co}^{\text{II}}(\text{Ch}_n)$ and $[\text{Co}^{\text{II}}(\text{Ch}_n\text{H})]^+$ (eq 4),

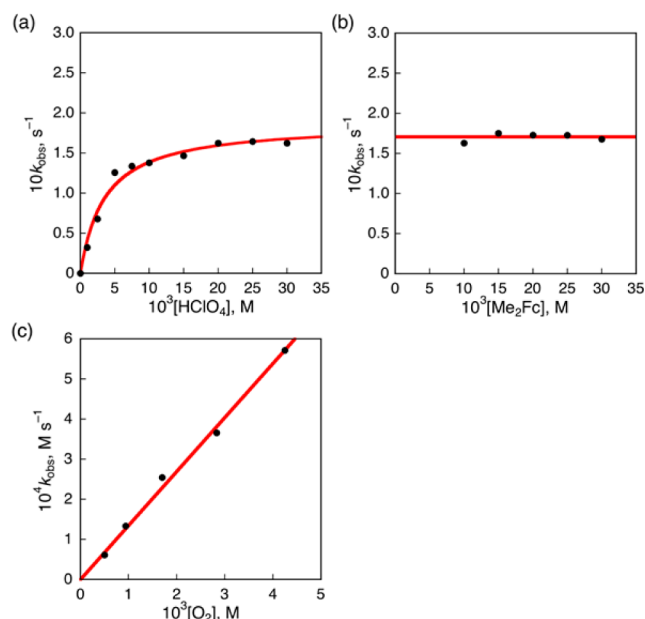
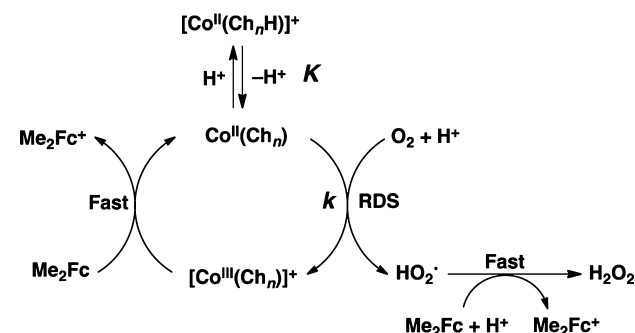


Figure 7. Plots of k_{obs} vs (a) $[\text{HClO}_4]$, (b) $[\text{Me}_2\text{Fc}]$, and (c) $[\text{O}_2]$ for the two-electron reduction of O_2 in PhCN at 298 K. Typical conditions: $\text{Co}^{\text{II}}(\text{Ch}_2)$ (4.0×10^{-6} M), O_2 (1.7×10^{-3} M), Me_2Fc (2.5×10^{-2} M), and HClO_4 (2.5×10^{-2} M).

Scheme 2. Catalytic Mechanism of O_2 Reduction with $\text{Co}^{\text{II}}(\text{Ch}_n)$, $n = 2, 3$



$$[\text{Co}^{\text{II}}(\text{Ch}_n)] = [\text{Co}^{\text{II}}(\text{Ch}_n)]_t / K[\text{HClO}_4] \quad (4)$$

the concentration of $\text{Co}^{\text{II}}(\text{Ch}_n)$ in eq 3 is rewritten by eq 5,

$$\frac{d[\text{Me}_2\text{Fc}^+]/dt = k_{\text{cat}(n)}[\text{Co}^{\text{II}}(\text{Ch}_n)]_t[\text{O}_2][\text{HClO}_4]}{(1 + K[\text{HClO}_4])} \quad (5)$$

where $\text{Co}^{\text{II}}(\text{Ch}_n)_t$ are the total concentrations of $\text{Co}^{\text{II}}(\text{Ch}_n)$ and $[\text{Co}^{\text{II}}(\text{Ch}_n\text{H})]^+$. Thus, by combining eqs 3 and 4, we obtain eq 5. The $k_{\text{obs}(n)}$ ($n = 2, 3$) value is given by eq 6,

$$k_{\text{obs}(n)} = k_{\text{cat}(n)}[\text{Co}^{\text{II}}(\text{Ch}_n)]_t[\text{HClO}_4]/(1 + K[\text{HClO}_4]) \quad (6)$$

which is consistent with saturation behaviors as a function of the concentration of HClO_4 as shown in Figures 7a and S9a in the Supporting Information.

In order to determine the $k_{\text{cat}(n)}$ values, eq 6 is rewritten by eq 7,

$$k_{\text{obs}(n)}^{-1} = 1/k_{\text{cat}(n)}[\text{Co}^{\text{II}}(\text{Ch}_n)]_t[\text{HClO}_4] + K/k_{\text{cat}(n)}[\text{Co}^{\text{II}}(\text{Ch}_n)]_t \quad (7)$$

which predicts a linear correlation between $k_{\text{obs}(n)}^{-1}$ and $[\text{HClO}_4]^{-1}$ as shown in Figure S12 in the Supporting Information. The $k_{\text{cat}(n)}$ and K values were determined from the slope and intercept of the linear plot of $k_{\text{obs}(n)}^{-1}$ vs $[\text{HClO}_4]^{-1}$ to be $9.6 \times 10^6 \text{ M}^{-2} \text{ s}^{-1}$ and $1.8 \times 10^2 \text{ M}^{-1}$ for $\text{Co}^{\text{II}}(\text{Ch}_2)$ and $2.2 \times 10^7 \text{ M}^{-2} \text{ s}^{-1}$ and 78 M^{-1} for $\text{Co}^{\text{II}}(\text{Ch}_3)$, respectively. These K values agree with the results determined from the protonation of $\text{Co}^{\text{II}}(\text{Ch}_n)$ titrated with HClO_4 as shown in Figure S4 in the Supporting Information. Such agreement of the K values determined from the titration of $\text{Co}^{\text{II}}(\text{Ch}_n)$ ($n = 2, 3$) with HClO_4 and catalytic conditions provides evidence of the deprotonation of $[\text{Co}^{\text{II}}(\text{Ch}_n\text{H})]^+$ to afford $\text{Co}^{\text{II}}(\text{Ch}_n)$ ($n = 2, 3$) as an intermediate in a pre-equilibrium step that is followed by rate-determining inner-sphere electron transfer from $\text{Co}^{\text{II}}(\text{Ch}_n)$ to O_2 coupled with proton transfer. This is also consistent with the conclusion that $[\text{Co}^{\text{III}}(\text{Ch}_n)]^+$ ($n = 2, 3$) hardly undergo the protonation as observed in Figure S5 in the Supporting Information, and hence, no change of the redox potential of $[\text{Co}^{\text{III}}(\text{Ch}_n)]^+/\text{Co}^{\text{II}}(\text{Ch}_n)$ ($n = 2, 3$) was observed as mentioned in Figure 4.⁵² Thus, the introduction of electron-withdrawing substituents on chlorin ligand resulted in the positive shift of redox potential, resulting in the rejection of protonation in the presence of HClO_4 due to lower basicity. In contrast to $\text{Co}^{\text{II}}(\text{Ch}_n)$ ($n = 2, 3$), $[\text{Co}^{\text{II}}(\text{Ch}_1\text{H})]^+$ formed by the protonation of $\text{Co}^{\text{II}}(\text{Ch}_1)$ in the presence of a large concentration of HClO_4 also acts as a reactive intermediate in catalytic O_2 reduction. However, one-electron oxidation potential of $\text{Co}^{\text{II}}(\text{Ch}_1)$ was changed from 0.37 V (vs SCE) to 0.48 V due to the protonation, leading slower catalysis. As a result, such a change in redox property resulted in the enhancement of the catalytic reactivity, where the observed rate constant (k_{obs}) value of $\text{Co}^{\text{II}}(\text{Ch}_3)$ was 36-fold larger than that of $\text{Co}^{\text{II}}(\text{Ch}_1)$.⁵³

CONCLUSION

We have conclusively demonstrated effects of changes in redox potential or configuration of cobalt chlorin complexes ($\text{Co}^{\text{II}}(\text{Ch}_n)$ ($n = 1-3$)) on the catalytic mechanism and activity of two-electron reduction of dioxygen (O_2). All of the cobalt chlorin complexes ($\text{Co}^{\text{II}}(\text{Ch}_n)$ ($n = 1-3$)) efficiently and selectively catalyzed two-electron reduction of O_2 by Me_2Fc to produce H_2O_2 in the presence of HClO_4 in PhCN at 298 K. The detailed kinetic studies have revealed that the rate-determining step in the catalytic cycle is the proton-coupled electron transfer from $\text{Co}^{\text{II}}(\text{Ch}_n)$ ($n = 2, 3$), which is in protonation equilibrium between $[\text{Co}^{\text{II}}(\text{Ch}_n\text{H})]^+$, to O_2 to produce $[\text{Co}^{\text{III}}(\text{Ch}_n)]^+$ ($n = 2, 3$) and HO_2^\bullet . The introduction of electron-withdrawing substituents on chlorin ligand resulted in the enhancement of catalytic reactivity, which is attributed to the more negative redox potential of $[\text{Co}^{\text{III}}(\text{Ch}_n)]^+/\text{Co}^{\text{II}}(\text{Ch}_n)$ ($n = 2, 3$) in the presence of HClO_4 due to lower acceptability of proton. In summary, the present study provides valuable insights toward the development of more efficient catalysts for the selective two-electron reduction of O_2 to produce H_2O_2 , which is a promising candidate for a renewable energy source.

ASSOCIATED CONTENT

Supporting Information

Spectroscopic and kinetic data. This material is available free of charge via the Internet at <http://pubs.acs.org>.

■ AUTHOR INFORMATION

Corresponding Author

*E-mail: fukuzumi@chem.eng.osaka-u.ac.jp.

Notes

The authors declare no competing financial interest.

■ ACKNOWLEDGMENTS

This work was supported by an Advanced Low Carbon Technology Research and Development (ALCA) program from Japan Science Technology Agency (JST) to S.F. and by Japan Society for the Promotion of Science (JSPS: 26620154 and 26288037 to K.O. and 25-727 to K.M.).

■ REFERENCES

- (1) (a) Rodriguez, C. A.; Modestino, M. A.; Psaltis, D.; Moser, C. *Energy Environ. Sci.* **2014**, *7*, 3828–3835. (b) Gu, S.; Xu, B.; Yan, Y. *Annu. Rev. Chem. Biomol. Eng.* **2014**, *5*, 429–454.
- (2) Luo, J.; Im, J.-H.; Mayer, M. T.; Schreier, M.; Nazeeruddin, M. K.; Park, N.-G.; Tilley, D.; Fan, H. J.; Grätzel, M. *Science* **2014**, *345*, 1593–1596.
- (3) (a) Fukuzumi, S.; Yamada, Y.; Karlin, K. D. *Electrochim. Acta* **2012**, *82*, 493–511. (b) Disselkamp, R. S. *Energy Fuels* **2008**, *22*, 2771–2774. (c) Disselkamp, R. S. *Int. J. Hydrogen Energy* **2010**, *35*, 1049–1053.
- (4) (a) Yamazaki, S.; Siroma, Z.; Senoh, H.; Ioroi, T.; Fujiwara, N.; Yasuda, K. *J. Power Sources* **2008**, *178*, 20–25. (b) Yamada, Y.; Fukunishi, Y.; Yamazaki, S.; Fukuzumi, S. *Chem. Commun.* **2010**, *46*, 7334–7336.
- (5) Sanli, A. E. *Int. J. Energy Res.* **2013**, *37*, 1488–1497.
- (6) (a) Shaegh, S. A. M.; Ehteshami, S. M. M.; Chan, S. H.; Nguyen, N.-T.; Tan, S. N. *RSC Adv.* **2014**, *4*, 37284–37287. (b) Shaegh, S. A. M.; Nguyen, N.-T.; Ehteshami, S. M. M.; Chan, S. H. *Energy Environ. Sci.* **2012**, *5*, 8225–8228.
- (7) Yang, F.; Cheng, K.; Xiao, X.; Yin, J.; Wang, G.; Cao, D. *J. Power Sources* **2014**, *245*, 89–94.
- (8) (a) Yamada, Y.; Fukuzumi, S. *Aust. J. Chem.* **2014**, *67*, 354–364. (b) Yamada, Y.; Yoneda, M.; Fukuzumi, S. *Inorg. Chem.* **2014**, *53*, 1272–1274. (c) Yamada, Y.; Yoneda, M.; Fukuzumi, S. *Chem.—Eur. J.* **2013**, *19*, 11733–11741. (d) Yamada, Y.; Yoshida, S.; Honda, T.; Fukuzumi, S. *Energy Environ. Sci.* **2011**, *4*, 2822–2825.
- (9) Santacesaria, E.; Serio, M. D.; Velotti, R.; Leone, U. *Ind. Eng. Chem. Res.* **1994**, *33*, 277–284.
- (10) Hoffman, A. J.; Carraway, E. R.; Hoffmann, M. R. *Environ. Sci. Technol.* **1994**, *28*, 776–785.
- (11) (a) Maurino, V.; Minero, C.; Mariella, G.; Pelizzetti, E. *Chem. Commun.* **2005**, 2627–2629. (b) Teranishi, M.; Naya, S.; Tada, H. *J. Am. Chem. Soc.* **2010**, *132*, 7850–7851. (c) Tsukamoto, D.; Shiro, A.; Shiraiishi, Y.; Sugano, Y.; Ichikawa, S.; Tanaka, S.; Hirai, T. *ACS Catal.* **2012**, *2*, 599–603.
- (12) Kato, S.; Jung, J.; Suenobu, T.; Fukuzumi, S. *Energy Environ. Sci.* **2013**, *6*, 3756–3764.
- (13) Shiraiishi, Y.; Kanazawa, S.; Kofuji, Y.; Sakamoto, H.; Ichikawa, S.; Tanaka, S.; Hirai, T. *Angew. Chem., Int. Ed.* **2014**, *53*, 13454–13459.
- (14) (a) Yamada, Y.; Nomura, A.; Ohkubo, K.; Suenobu, T.; Fukuzumi, S. *Chem. Commun.* **2013**, *49*, 5132–5134. (b) Yamada, Y.; Nomura, A.; Miyahigashi, T.; Fukuzumi, S. *Chem. Commun.* **2012**, *48*, 8329–8331.
- (15) (a) Fukuzumi, S.; Ohkubo, K. *Chem. Sci.* **2013**, *4*, 561–574. (b) Fukuzumi, S.; Ohkubo, K. *Org. Biomol. Chem.* **2014**, *12*, 6059–6071. (c) Ohkubo, K.; Fukuzumi, S. *Bull. Chem. Soc. Jpn.* **2009**, *82*, 303–315. (d) Kotani, H.; Ohkubo, K.; Fukuzumi, S. *Appl. Catal., B* **2008**, *77*, 317–324. (e) Ohkubo, K.; Iwata, R.; Mizushima, K.; Souma, K.; Yamamoto, Y.; Suzuki, N.; Fukuzumi, S. *Chem. Commun.* **2010**, *46*, 601–603. (f) Ohkubo, K.; Kobayashi, T.; Fukuzumi, S. *Angew. Chem., Int. Ed.* **2011**, *50*, 8652–8655.
- (16) Fukushima, M.; Tatsumi, K.; Tanaka, S.; Nakamura, H. *Environ. Sci. Technol.* **1998**, *32*, 3948–3953.
- (17) Liu, S.; Mase, K.; Bougher, C.; Hicks, S. D.; Abu-Omar, M. M.; Fukuzumi, S. *Inorg. Chem.* **2014**, *53*, 7780–7788.
- (18) Mase, K.; Ohkubo, K.; Fukuzumi, S. *J. Am. Chem. Soc.* **2013**, *135*, 2800–2808.
- (19) (a) Honda, T.; Kojima, T.; Fukuzumi, S. *J. Am. Chem. Soc.* **2012**, *134*, 4196–4206. (b) Fukuzumi, S. *Chem. Lett.* **2008**, *37*, 808–813. (c) Fukuzumi, S.; Okamoto, K.; Gros, C. P.; Guillard, R. *J. Am. Chem. Soc.* **2004**, *126*, 10441–10449. (d) Fukuzumi, S.; Okamoto, K.; Tokuda, Y.; Gros, C. P.; Guillard, R. *J. Am. Chem. Soc.* **2004**, *126*, 17059–17066.
- (20) (a) Fukuzumi, S.; Mochizuki, S.; Tanaka, T. *Inorg. Chem.* **1989**, *28*, 2459–2465. (b) Fukuzumi, S.; Mochizuki, S.; Tanaka, T. *Inorg. Chem.* **1990**, *29*, 653–659. (c) Fukuzumi, S.; Mochizuki, S.; Tanaka, T. *J. Chem. Soc., Chem. Commun.* **1989**, 391–392.
- (21) (a) McGuire, R., Jr.; Dogutan, D. K.; Teets, T. S.; Suntovich, J.; Shao-Horn, Y.; Nocera, D. G. *Chem. Sci.* **2010**, *1*, 411–414. (b) Dogutan, D. K.; Stoian, S. A.; McGuire, R., Jr.; Schwalbe, M.; Teets, T. S.; Nocera, D. G. *J. Am. Chem. Soc.* **2011**, *133*, 131–140. (c) Teets, T. S.; Cook, T. R.; McCarthy, B. D.; Nocera, D. G. *J. Am. Chem. Soc.* **2011**, *133*, 8114–8117.
- (22) (a) Anson, F. C.; Shi, C.; Steiger, B. *Acc. Chem. Res.* **1997**, *30*, 437–444. (b) Shi, C.; Steiger, B.; Yuasa, M.; Anson, F. C. *Inorg. Chem.* **1997**, *36*, 4294–4295. (c) Shi, C. N.; Anson, F. C. *Inorg. Chem.* **1998**, *37*, 1037–1043. (d) Liu, Z.; Anson, F. C. *Inorg. Chem.* **2000**, *39*, 274–280.
- (23) (a) Schechter, A.; Stanevsky, M.; Mahammed, A.; Gross, Z. *Inorg. Chem.* **2012**, *51*, 22–24. (b) Masa, J.; Ozoemena, K.; Schuhmann, W.; Zagal, J. H. *J. Porphyryns Phthalocyanines* **2012**, *16*, 761–784. (c) Zagal, J. H.; Griveau, S.; Silva, J. F.; Nyokong, T.; Bedioui, F. *Coord. Chem. Rev.* **2010**, *254*, 2755–2791.
- (24) (a) Olaya, A. J.; Schaming, D.; Brevet, P.-F.; Nagatani, H.; Zimmermann, T.; Vanicek, J.; Xu, H.-J.; Gros, C. P.; Barbe, J.-M.; Girault, H. H. *J. Am. Chem. Soc.* **2012**, *134*, 498–506. (b) Peljo, P.; Murtomäki, L.; Kallio, T.; Xu, H.-J.; Meyer, M.; Gros, C. P.; Barbe, J.-M.; Girault, H. H.; Laasonen, K.; Kontturi, K. *J. Am. Chem. Soc.* **2012**, *134*, 5974–5984. (c) Su, B.; Hatay, I.; Trojanek, A.; Samec, Z.; Khoury, T.; Gros, C. P.; Barbe, J.-M.; Daina, A.; Carrupt, P.-A.; Girault, H. H. *J. Am. Chem. Soc.* **2010**, *132*, 2655–2662.
- (25) (a) Fukuzumi, S.; Mandal, S.; Mase, K.; Ohkubo, K.; Park, H.; Benet-Buchholz, J.; Nam, W.; Llobet, A. *J. Am. Chem. Soc.* **2012**, *134*, 9906–9909. (b) Wada, T.; Maki, H.; Imamoto, T.; Yuki, H.; Miyazato, Y. *Chem. Commun.* **2013**, *49*, 4394–4396.
- (26) (a) Sun, B.; Ou, Z.; Meng, D.; Fang, Y.; Song, Y.; Zhu, W.; Solntsev, P. V.; Nemykin, V. N.; Kadish, K. M. *Inorg. Chem.* **2014**, *53*, 8600–8609. (b) Kadish, K. M.; Fremont, L.; Shen, J.; Chen, P.; Ohkubo, K.; Fukuzumi, S.; El Ojaimi, M.; Gros, C. P.; Barbe, J. M.; Guillard, R. *Inorg. Chem.* **2009**, *48*, 2571–2582. (c) Chen, P.; Lau, H.; Habermeyer, B.; Gros, C. P.; Barbe, J. M.; Kadish, K. M. *J. Porphyryns Phthalocyanines* **2011**, *15*, 467–479. (d) Kadish, K. M.; Shen, J.; Frémond, C.; Chen, P.; Ojaimi, M. E.; Chkounda, M.; Gros, C. P.; Barbe, J.-M.; Ohkubo, K.; Fukuzumi, S.; Guillard, R. *Inorg. Chem.* **2008**, *47*, 6726–6737. (e) Kadish, K. M.; Fremont, L.; Ou, Z.; Shao, J.; Shi, C.; Anson, F. C.; Burdet, F.; Gros, C. P.; Barbe, J.-M.; Guillard, R. *J. Am. Chem. Soc.* **2005**, *127*, 5625–5631. (f) D'Souza, F.; Villard, A.; Caemelbecke, E. V.; Franzen, M.; Boschi, T.; Tagliatesta, P.; Kadish, K. M. *Inorg. Chem.* **1993**, *32*, 4042–4048.
- (27) (a) Chang, C. J.; Deng, Y.; Nocera, D. G.; Shi, C.; Anson, F. C.; Chang, C. K. *Chem. Commun.* **2000**, 1355–1356. (b) Chang, C. J.; Loh, Z. H.; Shi, C.; Anson, F. C.; Nocera, D. G. *J. Am. Chem. Soc.* **2004**, *126*, 10013–10020.
- (28) (a) Askarizadeh, E.; Yaghoob, S. B.; Boghaei, D. M.; Slawin, A. M.; Love, J. B. *Chem. Commun.* **2010**, *46*, 710–712. (b) Volpe, M.; Hartnett, H.; Leeland, J. W.; Wills, K.; Ogunshun, M.; Duncombe, B. J.; Wilson, C.; Blake, A. J.; McMaster, J.; Love, J. B. *Inorg. Chem.* **2009**, *48*, 5195–5207.
- (29) (a) Decréau, R. A.; Collman, J. P.; Hosseini, A. *Chem. Soc. Rev.* **2010**, *39*, 1291–1301. (b) Collman, J. P.; Boulatov, R.; Sunderland, C. J.; Fu, L. *Chem. Rev.* **2004**, *104*, 561–588.

- (30) (a) Rosenthal, J.; Nocera, D. G. *Acc. Chem. Res.* **2007**, *40*, 543–553. (b) Schwalbe, M.; Dogutan, D. K.; Stoian, S. A.; Teets, T. S.; Nocera, D. G. *Inorg. Chem.* **2011**, *50*, 1368–1377. (c) Chang, C. J.; Chng, L. L.; Nocera, D. G. *J. Am. Chem. Soc.* **2003**, *125*, 1866–1876.
- (31) (a) Halime, Z.; Kotani, H.; Li, Y.; Fukuzumi, S.; Karlin, K. D. *Proc. Natl. Acad. Sci. U.S.A.* **2011**, *108*, 13990–13994. (b) Chufan, E. E.; Puiu, S. C.; Karlin, K. D. *Acc. Chem. Res.* **2007**, *40*, 563–572. (c) Kim, E.; Chufan, E. E.; Kamaraj, K.; Karlin, K. D. *Chem. Rev.* **2004**, *104*, 1077–1133.
- (32) (a) Wasylenko, D. J.; Rodríguez, C.; Pegis, M. L.; Mayer, J. M. *J. Am. Chem. Soc.* **2014**, *136*, 12544–12547. (b) Carver, C. T.; Matson, B. D.; Mayer, J. M. *J. Am. Chem. Soc.* **2012**, *134*, 5444–5447. (c) Matson, B. D.; Carver, C. T.; Von Ruden, A.; Yang, J. Y.; Raugei, S.; Mayer, J. M. *Chem. Commun.* **2012**, *48*, 11100–11102. (d) Warren, J. J.; Tronic, T. A.; Mayer, J. M. *Chem. Rev.* **2010**, *110*, 6961–7001.
- (33) (a) Kakuda, S.; Peterson, R. L.; Ohkubo, K.; Karlin, K. D.; Fukuzumi, S. *J. Am. Chem. Soc.* **2013**, *135*, 6513–6522. (b) Das, D.; Lee, Y.-M.; Ohkubo, K.; Nam, W.; Karlin, K. D.; Fukuzumi, S. *J. Am. Chem. Soc.* **2013**, *135*, 2825–2834. (c) Das, D.; Lee, Y.-M.; Ohkubo, K.; Nam, W.; Karlin, K. D.; Fukuzumi, S. *J. Am. Chem. Soc.* **2013**, *135*, 4018–4026. (d) Fukuzumi, S.; Tahsini, L.; Lee, Y.-M.; Ohkubo, K.; Nam, W.; Karlin, K. D. *J. Am. Chem. Soc.* **2012**, *134*, 7025–7035.
- (34) (a) Fukuzumi, S.; Karlin, K. D. *Coord. Chem. Rev.* **2013**, *257*, 187–195. (b) Tahsini, L.; Kotani, H.; Lee, Y.-M.; Cho, J.; Nam, W.; Karlin, K. D.; Fukuzumi, S. *Chem.—Eur. J.* **2012**, *18*, 1084–1093. (c) Fukuzumi, S.; Kotani, H.; Lucas, H. R.; Doi, K.; Suenobu, T.; Peterson, R. L.; Karlin, K. D. *J. Am. Chem. Soc.* **2010**, *132*, 6874–6875.
- (35) (a) Zhang, J.; Anson, F. C. *J. Electroanal. Chem.* **1993**, *348*, 81–97. (b) Lei, Y.; Anson, F. C. *Inorg. Chem.* **1994**, *33*, 5003–5009. (c) Weng, Y. C.; Fan, F.-R. F.; Bard, A. J. *J. Am. Chem. Soc.* **2005**, *127*, 17576–17577.
- (36) (a) Thorum, M. S.; Yadav, J.; Gewirth, A. A. *Angew. Chem., Int. Ed.* **2009**, *48*, 165–167. (b) McCrory, C. C. L.; Devadoss, A.; Ottenwaelder, X.; Lowe, R. D.; Stack, T. D. P.; Chidsey, C. E. D. *J. Am. Chem. Soc.* **2011**, *133*, 3696–3699. (c) Thorseth, M. A.; Tornow, C. E.; Tse, E. C. M.; Gewirth, A. A. *Coord. Chem. Rev.* **2013**, *257*, 130–139. (d) Thorseth, M. A.; Letko, C. S.; Rauchfuss, T. B.; Gewirth, A. A. *Inorg. Chem.* **2011**, *50*, 6158–6162.
- (37) Orzel, E.; Kania, A.; Rutkowska-Żbik, D.; Susz, A.; Stochel, G.; Fiedor, L. *Inorg. Chem.* **2010**, *49*, 7362–7371.
- (38) Chen, C.-Y.; Sun, E.; Fan, D.; Taniguchi, M.; McDowell, B. E.; Yang, E.; Diers, J. R.; Bocian, D. F.; Holten, D.; Lindsey, J. S. *Inorg. Chem.* **2012**, *51*, 9443–9464.
- (39) Saga, Y.; Miura, R.; Sadaoka, K.; Hirai, Y. *J. Phys. Chem. B* **2011**, *115*, 11757–11762.
- (40) (a) Oettmeler, W.; Janson, T. R.; Thurnauer, M. C.; Shipman, L. L.; Katz, J. J. *J. Phys. Chem.* **1977**, *81*, 339–342. (b) Hartwich, G.; Fiedor, L.; Simonin, I.; Cmiel, E.; Schäfer, W.; Noy, D.; Scherz, A.; Scheer, H. *J. Am. Chem. Soc.* **1998**, *120*, 3675–3683.
- (41) Armarego, W. L. F.; Chai, C. L. L. *Purification of Laboratory Chemicals*, 7th ed; Pergamon Press: Oxford, 2013.
- (42) (a) Wasieleski, M. R.; Svec, W. A. *J. Org. Chem.* **1980**, *45*, 1969–1974. (b) Zheng, G.; Li, H.; Zhang, M.; L-Katz, S.; Chance, B.; Glickson, J. D. *Bioconjugate Chem.* **2002**, *13*, 392–396. (c) Arian, D.; Cló, E.; Gothelf, K. V.; Mokhir, A. *Chem.—Eur. J.* **2010**, *16*, 288–295. (d) Ishigure, S.; Mitsui, T.; Ito, S.; Kondo, Y.; Kawabe, S.; Kondo, M.; Dewa, T.; Mino, H.; Itoh, S.; Nango, M. *Langmuir* **2010**, *26*, 7774–7782. (e) Paolesse, R.; Pandey, R. K.; Forsyth, T. P.; Jaquinod, L.; Gerzevske, K. R.; Nurco, D. J.; Senge, M. O.; Licoccia, S.; Boschi, T.; Smith, K. M. *J. Am. Chem. Soc.* **1996**, *118*, 3869–3882.
- (43) (a) Tamiaki, H.; Kunieda, M. *J. Org. Chem.* **2007**, *72*, 2443–2451. (b) Huber, V.; Sengupta, S.; Würthner, F. *Chem.—Eur. J.* **2008**, *14*, 7791–7807.
- (44) Tamiaki, H.; Miyata, S.; Kureishi, Y.; Tanikaga, R. *Tetrahedron* **1996**, *52*, 12421–12432.
- (45) Tamiaki, H.; Amakawa, M.; Shimono, Y.; Tanikaga, R.; Holzwarth, A. R.; Schaffner, K. *Photochem. Photobiol.* **1996**, *63*, 92–99.
- (46) (a) Ellis, P. E.; Linard, J. E.; Szymanski, T.; Jones, R. D.; Budge, J. R.; Basolo, F. J. *Am. Chem. Soc.* **1980**, *102*, 1889–1896. (b) Hill, A. V. *J. Physiol. (London)* **1910**, *40*, 4–7.
- (47) Fukuzumi, S.; Kuroda, S.; Tanaka, T. *J. Am. Chem. Soc.* **1985**, *107*, 3020–3027.
- (48) (a) Fukuzumi, S.; Imahori, H.; Yamada, H.; El-Khouly, M. E.; Fujitsuka, M.; Ito, O.; Guldi, D. M. *J. Am. Chem. Soc.* **2001**, *123*, 2571–2575. (b) Fukuzumi, S.; Ishikawa, M.; Tanaka, T. *J. Chem. Soc., Perkin Trans. 2* **1989**, 1037–1045.
- (49) Mann, C. K.; Barnes, K. K. In *Electrochemical Reactions in Non-aqueous Systems*; Marcel Dekker: New York, 1970.
- (50) Lin, X. Q.; Boisselier-Cocolios, B.; Kadish, K. M. *Inorg. Chem.* **1986**, *25*, 3242–3248.
- (51) Time profiles of absorbance at 650 nm due to formation of Me_2Fc^+ by changing the concentration of $\text{Co}^{\text{II}}(\text{Ch}_n)$ ($n = 2, 3$), HClO_4 , Me_2Fc , and O_2 are shown in Figures S7 and S10 in the Supporting Information, respectively. Pseudo-first-order plots of time profiles of absorbance at 650 nm are shown in Figures S8 and S11 in the Supporting Information, respectively.
- (52) These are in contrast to the previously reported results that the rate-determining step of O_2 reduction catalyzed by $\text{Co}^{\text{II}}(\text{Ch}_1)$ is proton-coupled electron transfer (PCET) from $\text{Co}^{\text{II}}(\text{Ch}_1)$ to O_2 to produce $[\text{Co}^{\text{III}}(\text{Ch}_1)]^+$ and HO_2^\bullet , where $[\text{Co}^{\text{II}}(\text{Ch}_1\text{H})]^+$ formed by the protonation of $\text{Co}^{\text{II}}(\text{Ch}_1)$ in the presence of the large concentration of HClO_4 also catalyzes O_2 reduction; see ref 18.
- (53) It has been reported that MN4 metal complexes with more positive redox potential show higher reactivity in an electrocatalytic reduction of O_2 .^{23c} However, the enhancement in the catalytic reactivity by the introduction of an electron-withdrawing group is associated with the decrease in the proton acceptability of carbonyl group (position C-13¹), which results in the more negative redox potential of $[\text{Co}^{\text{III}}(\text{Ch}_n)]^+/\text{Co}^{\text{II}}(\text{Ch}_n)$ ($n = 2, 3$) under acidic conditions.